Research Article

Journal of RAMAN SPECTROSCOPY

Received: 5 March 2011 Revised: 2 September 2011 Accepted: 3 September 2011 Published online in Wiley Online Library: 27 October 2011

(wileyonlinelibrary.com) DOI 10.1002/jrs.3071

Raman scattering study of temperature and hydrostatic pressure phase transitions in Rb_2KTiOF_5 crystal

A. S. Krylov,[a] S. V. Goryainov,[b] A. N. Vtyurin,[a] S. N. Krylova,[a]* S. N. Sofronova,[a] N. M. Laptash,[c] T. B. Emelina,[c] V. N. Voronov[a] and S. V. Babushkin[a]

Raman spectra of Rb_2KTiOF_5 crystal were obtained and analyzed in the temperature range from 77 to 297 K and under hydrostatic pressure up to 4.2 GPa (at $T = 295$ K). The experimental results were compared with quantum-chemical simulation of $TiOF_5$ pseudo-octahedron. To interpret effects of lattice ordering, phonon spectra of several ordered phases of Rb_2KTiOF_5 were calculated within *ab initio* generalized Gordon–Kim model, and ordering of $TiOF_5$ molecular groups were simulated within Monte Carlo approach. The spectra exhibited orientation disordering in the cubic phase under ambient conditions. Cooling below the phase transition temperature (215 K) leads to partial ordering of the structure. The isotropic perovskite-like phase was found to undergo first-order transition into a low-symmetry anisotropic phase at about 1 GPa. Further compression up to 4.1 GPa did not show any effects associated with phase transitions. Copyright © 2011 John Wiley & Sons, Ltd.

Supporting information may be found in the online version of this article.

Keywords: structural phase transition; Rb_2KTiOF_5; Raman spectroscopy; hysteresis; hydrostatic pressure

Introduction

At room temperature, Rb_2KTiOF_5 compound crystallizes into an elpasolite-type structure of cubic syngony.[1] The crystalline, ceramic, and film materials with perovskite-like structures are widely used as functional elements because of their remarkable properties. Temperature and pressure changes in oxyfluorides,[2–10] cause a number of anomalous structural phase transitions, which are generally related to changes in the lattice of octahedral groups, such as small pivoting of these octahedra or their orientational ordering. Because of significant entropy and caloric effects these compounds are used as active elements in solid-state cooling systems. Electrocaloric effects in these materials were reviewed by Scott and Blinc[2,3] and barocaloric effects in the perovskite-like structures were studied by Flerov *et al.*[8]

The crystal Rb_2KTiOF_5 belongs to a family of crystals with general formula $A_2BMO_xF_{6-x}$, where A, B – K, Rb, Cs, NH_4; M – W, Mo, Ti, Nb, Ta, and $x = 1, 2, 3$ depends on the valence of central atom M. These compounds crystallize in cubic syngony into an elpasolite-type structure (space group $Fm\bar{3}m$, $Z = 4$)[1] displayed in Fig. S1. Obviously, to keep cubic symmetry intact, the orientations of MO_xF_{6-x} pseudo-octahedral groups should be disordered. Pseudo-octahedral fluorine–oxygen anions are polar because of different charges of oxygen and fluorine atoms and displacement of the central atom toward oxygen atoms.

Crystallochemical and structural analysis proved that at room temperature the structure of $[MOF_5]$ ion-based elpasolites with general formula A_2BMOF_5 (A, B = Li, Na, K, Rb, Cs) is cubic.[11–14] Infrared spectroscopy of titanium-containing oxyfluorides showed the symmetry of $TiOF_5$ anion to be tetragonal C_{4v}.[14]

Effects of hydrostatic pressure on transition temperature in Rb_2KTiOF_5 have been studied previously only up to 0.6 GPa.[4] It was shown that an increase in hydrostatic pressure increases temperature of transition from cubic phase and expands stability range of the tetragonal phase. Gorev and colleagues[6–8] observed barocaloric effect in the Rb_2KTiOF_5 crystal.

The studies of phase transitions in Rb_2KTiOF_5 under cooling[4] have shown the transition at $T = 215$ K from phase G_0 ($Fm\bar{3}m$) into phase G_1 (probably $I/4m$), which was largely because of $TiOF_5$ octahedra ordering. Calorimetric studies have shown that this transition is accompanied by considerable entropy changes[4] ($S \approx R\ln 8$), typical for the order–disorder transformations. Temperature phase transitions were also observed in a similar structure $(NH_4)_3TiOF_5$.[11,12] The processes of orientational ordering in $(NH_4)_3TiOF_5$ crystal was found to have considerable effect on positions and widths of Raman lines.

In this article, we present experimental investigations of Raman spectra of polycrystals and small unoriented Rb_2KTiOF_5 crystals in the temperature range from 77 to 297 K and under hydrostatic pressure up to 4.2 GPa. The comparison of experimental results with theoretical calculations accomplished to define the role of molecular groups $TiOF_5^{3-}$ in the mechanism of phase transitions.

* *Correspondence to: S. N. Krylova, Kirensky Institute of Physics, 660036, Krasnoyarsk, Russia. E-mail: slanky@iph.krasn.ru*

a *Kirensky Institute of Physics, 660036, Krasnoyarsk, Russia*

b *Institute of Mineralogy and Petrogaphy, 630090, Novosibirsk, Russia*

c *Institute of Chemistry, 690022, Vladivostok, Russia*

Experimental Methods and Data Processing

The microcrystalline powder of Rb_2KTiOF_5 was synthesized by a solid phase reaction. The samples were taken from the same crystallization as described by Fokina *et al*.[4]

Raman spectra were collected in a backscattering geometry, using a triple monochromator Jobin Yvon T64000 Raman spectrometer operating in double subtractive mode then detected by a charge-coupled device cooled at 140 K. The spectral resolution for the recorded Stokes side Raman spectra was set to ~1 cm^{-1} (this resolution was achieved by using gratings with 1800 grooves mm^{-1} and 100 μm slits). The microscope system based on Olympus BX41 microscope with a 50× objective lens $f = 10.6$ mm with 0.5 numerical aperture provides a focal spot diameter of about 5 μm on the sample. Single-mode argon 514.5 nm from a Spectra-Physics Stabilite 2017 Ar^+ laser of 100 mW power (15 mW on the sample) was used as excitation light source. The intensity of the laser light was adjusted to avoid sample heating.

Temperature studies were performed in a LINKAM TMS-94-controlled LINKAM THMS-600 microchamber in a range from 77 to 297 K. The accuracy of sample temperature stabilization during measurements was within 0.1 K.

High-pressure experiments (up to 4.2 GPa) were performed at 295 K in a diamond anvil cell. More details can be found in Ref.[15] A thoroughly dehydrated 1:4 methanol–ethanol mixture was used as a pressure-transmitting medium. Small unoriented microcrystal samples with size 70–80 μm were placed in a chamber 250 μm in diameter and 100 μm thick. Pressure was monitored by the shift of the $^2F_g \rightarrow {}^4A_{2g}$ fluorescence band of Cr^{3+} ion in a small ruby crystal placed in the vicinity of the sample[16–18] within the experimental error about 0.05 GPa. Domain structure and birefringence effects were observed at the same time with a polarization microscope. All measurements made under pressure were reproduced on different samples taken in the same crystallization.

To obtain quantitative information about spectral line parameters, their profiles were deconvoluted employing the Voigt profile.[19] The effects that give rise to a Gaussian line shape, such as instrumental and Doppler broadening, tend to be independent of those contributing to a Lorentzian shape, such as natural or collisional broadening. Convolution of these two types of functions results in a Voigt profile where both types of broadening could be taken into account.

Experimental Results and Discussion

Phase transitions with temperature changes

Experimental transformation Raman spectra with temperature are shown in Fig. 1. The spectrum can be divided into several regions: low-wavenumber lattice vibrations, the rubidium displacements region — 10–150 cm^{-1}, medium-wavenumber region of $TiOF_5^{3-}$ ions internal vibrations (Ti–F stretching and bending modes) — 150–550 cm^{-1}, and 700–1000 cm^{-1} region, which contains lines corresponding to Ti–O stretching mode of $TiOF_5^{3-}$ ions. Red curves (288 K, 218 K) in Fig. 1 correspond to the cubic phase, and blue curves (178 K, 77 K) to the tetragonal phase. The origin of the band 670 cm^{-1} bound to partial hydroliysis of a sample surface. This band existence and intensity depend on sample history.

To attribute lines of $TiOF_5^{3-}$ internal vibrations, we performed a quantum-chemical simulation of an isolated ion. The symmetry types, internal mode frequencies, and eigenvectors of $[TiOF_5]^{3-}$

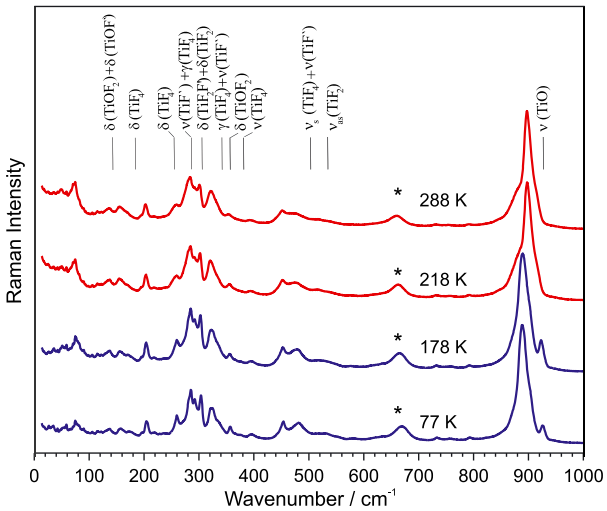

Figure 1. Raman spectra of Rb_2KTiOF_5 crystal at temperatures 77, 178, 218, and 288 K. Correlation of quantum-chemical calculation with experimental Raman spectrum. This figure is available in colour online at wileyonlinelibrary.com/journal/jrs.

complex were calculated employing GAMESS quantum-chemical software[20] within the density functional theory framework with exchange-correlation potential Becke, three-parameter, Lee–Yang–Parr. The 631 G basis set was used for the titanium atom and 6311 G basis set for light atoms (O, F). Optimization of geometric parameters of $[TiOF_5]^{3-}$ complex with local symmetry C_{4v} yielded the following distances in the quasi-octahedron: d (Ti–O) = 1.703 Å, d (Ti–F) = 1.988 Å, d (Ti–F′) = 2.087 Å, which were used to calculate the vibrational spectrum. The comparison of experimental and calculated spectra is presented in Table 1 and in Fig. 1. The notation of calculated wavenumbers is located at the upper part of Fig. 1. The main changes with decreasing temperature take place in the region of 850–950 cm^{-1}. At room temperature the spectrum here consists of three lines: 910, 897, and 881 cm^{-1}.

Dependence of this band components positions with temperature is shown in Fig. 2(a). The line at 881 cm^{-1} is denoted by triangles, line at 897 cm^{-1} by squares, and at 910 cm^{-1} by circles. Red marks correspond to temperature increase and blue ones to temperature decrease. Below the phase transition, the line at 910 cm^{-1} shifts upwards to 923 cm^{-1} and the line at 897 cm^{-1} shifts down to 890 cm^{-1}. The third line, 881 cm^{-1}, shifts to 870 cm^{-1} and broadens considerably; because of this broadening, assignment of this line position below 200 K becomes impossible. We found considerable (about 6 K) hysteresis of line shifts at the transition point. This is in good agreement with available calorimetry data.[4] According to quantum-chemical calculations, the region near 900 cm^{-1} corresponds to nondegenerated ν_1(TiO) vibration of free $TiOF_5^{3-}$ ion. The same interpretation of a similar band was found in the relaxor ferroelectrics.[21] Quantum-chemical calculations predict only one line in this wavenumber range, namely A_{1g} mode of Ti–O stretching (Table 1). In our experiments we observed three lines in this region both above and below the phase transition point. The appearance of these intense extra lines may be due to lattice disorder, resulting in different surroundings of $TiOF_5^{3-}$ ions. Figure 2(b) shows dependence of linewidths *versus* temperature. The same as in Fig. 2(a), the red color corresponds to sample heating and the blue one to sample cooling. The large width (25 cm^{-1}) of the line at 900 cm^{-1} in the distorted low temperature phase indicates that the octahedral ions remain partly disordered. This is in

Table 1. Experimental and calculated Raman spectrum of $TiOF_5^{3-}$ group

Symmetry type	Eigenvector	Notation	GAMESS calculation (cm^{-1})	Experiment, at 300 K (cm^{-1})
A_1	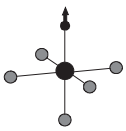	ν (TiO)	922	897
E	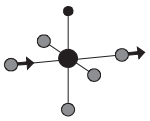	ν_{as} (TiF_2)	522	524, 471, 451
A_1	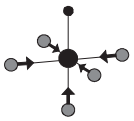	$\nu_s(TiF_4) + \nu(TiF')$	491	
B_2	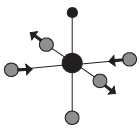	ν (TiF_4)	378	357, 335, 323
E	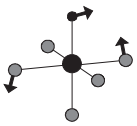	$\delta(TiOF_2)$	352	
A_1	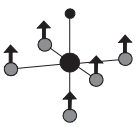	$\gamma(TiF_4) + \nu(TiF')$	346	
E	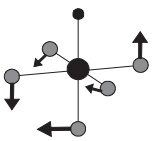	$\delta(TiF_2F') + \delta(TiF_2)$	305	302, 290, 286, 259
A_1	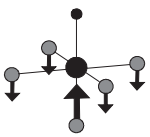	ν (TiF′) + $\gamma(TiF_4)$	284	
B_1	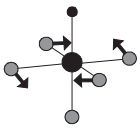	δ (TiF_4)	255	
B_2	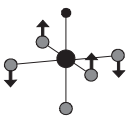	δ (TiF_4)	186	205, 157, 170, 136
E	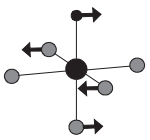	δ ($TiOF_2$) + δ(TiOF′)	149	

agreement with the model of distorted phase structure proposed by Fokina *et al.*[4] The width of this line may be attributed to phonon anharmonicity and lattice disorder, but such a large value and its weak temperature dependence indicate that disorder is the main factor, and it remains intact under further cooling.

The middle region of the Raman spectrum, 150–680 cm^{-1}, corresponds to Ti–F stretching and bending modes. Temperature dependencies of these line positions are shown in Fig. 3. As the temperature decreases the lines in the range 310–330 cm^{-1} shift slightly. Calculated data (Table 1) and experimental spectrum in this region are compared in Fig. 1. From the figure it is apparent that the position of these lines match the calculated vibration wavenumbers of Ti–F bonds and bending modes of these groups.

In the low-wavenumber region of the spectrum of the high temperature phase (Fig. 4(a)), the central peak has a wide wing up to 90 cm^{-1}, which may be indicative of lattice positional

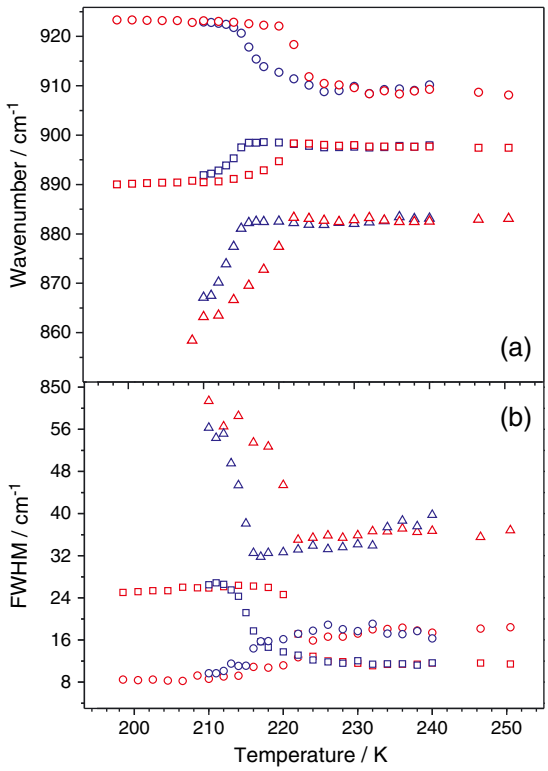

Figure 2. (a) Raman shift of spectrum lines *versus* temperature in range 850– 930 cm^{-1} and (b) temperature dependence full width at half-maximum of Raman spectrum lines in 850–930 cm^{-1} range. This figure is available in colour online at wileyonlinelibrary.com/journal/jrs.

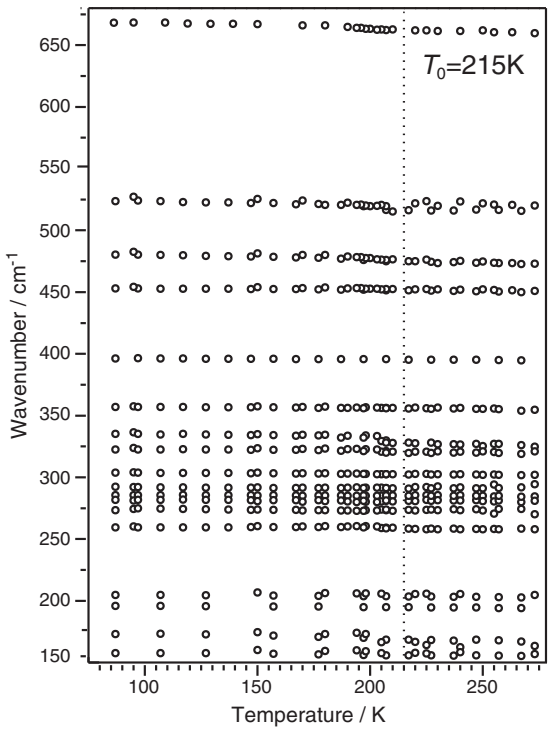

Figure 3. Raman shift of spectrum lines *versus* temperature in range 150–675 cm^{-1}.

disordering. In ordered elpasolites only one lattice mode is known to be active in this region, which corresponds to Rb^+ vibrations.[9,10] Two lines observed in current experiments may

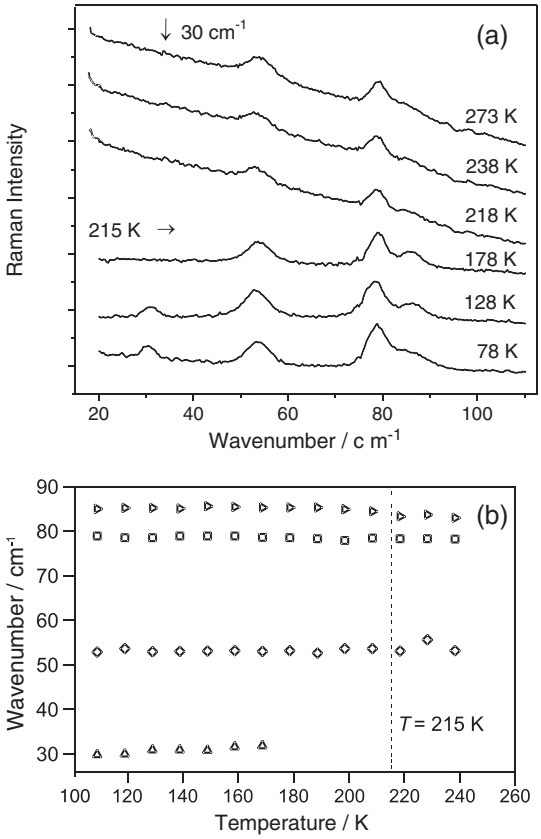

Figure 4. (a) Raman spectrum of Rb_2KTiOF_5 crystal in region 20–120 cm^{-1} at temperatures 78, 128, 178, 218, 238, and 273 K and (b) Raman shift of spectrum lines *versus* temperature in 20–100 cm^{-1} range.

be attributed to Rb^+ ions in a different environments. As the crystal cools below the transition point the width of these lines decreases and the wing disappears. Temperature dependencies of line positions in this region are given in Fig. 4(b). The position of the line at 82 cm^{-1} (at 273 K) shifts to 85 cm^{-1} (at 100 K). The lines presented in Figs 4(a) and (b) are damped and smeared by a tail of central peak. Therefore, such a small frequency shift cannot be discussed accurately. Below 170 K a new line was observed in the 30 cm^{-1} region; however, no soft mode behavior was found for this line. We assume that this anomalous line is irrelevant to phase transition. Similar anomalies were previously reported by Ya. Kavun *et al.* at 150 K[22] and Voigt *et al.* at 163 K.[5] Fokina *et al.*[4] suggested that this anomaly is due to the coexistence of cubic and tetragonal phases.

Phase transition under pressure

The transformation spectra under compression are shown in Fig. 5(a). At the ambient-pressure the high frequency band consists of three lines: 905, 897, and 880 cm^{-1}. The fitting spectra for some pressures shown in Fig. S2. Blue lines indicate the about 880 cm^{-1} mode, green lines indicate the about 897 cm^{-1} mode, pink lines indicate the about 905 cm^{-1} mode. Red lines reproduce the spectra in the wavenumber region above 800 cm^{-1}.

The dependencies of Ti–O stretching positions *versus* pressure are plotted in Fig. 5(b). They move up evenly, and after the pressure reaches 1 GPa, the growth rate decreases. At the same point the microphotographs show the appearance of optical anisotropy of the sample. Temperature dependences

Journal of RAMAN SPECTROSCOPY

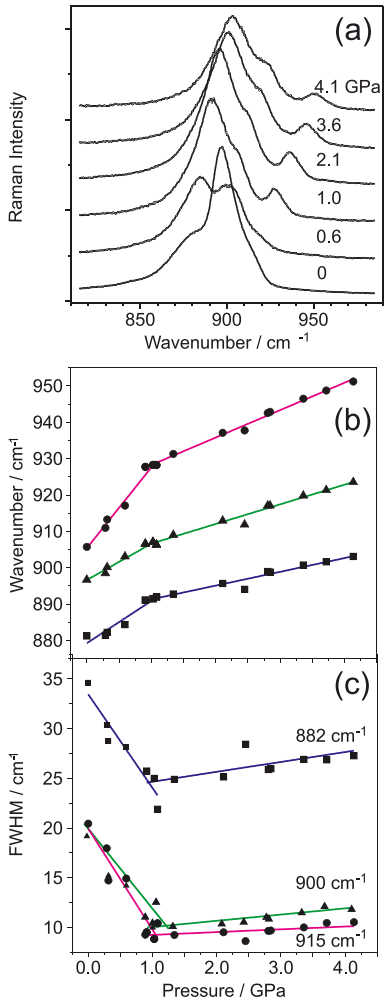

Figure 5. (a) Transformation of Raman spectra with pressure in range 810 – 990 cm^{-1}; (b) Raman shift of Ti–O vibrations *versus* pressure; and (c) full width at half-maximum of Ti–O vibrations *versus* pressure. This figure is available in colour online at wileyonlinelibrary.com/journal/jrs.

of the same band components positions (Fig. 2(a)) demonstrate a quite different behavior.

The dependences of widths of Ti–O vibrations versus pressure are plotted in Fig. 5(c). Considerable decrease of linewidths for the lines of Ti–O vibrations at a pressure above 1 GPa is indicative of phase transition. The dependencies of the band components widths with temperature (Fig. 2(b)) differ from their dependencies under compression (Fig. 5(c)). No hysteresis phenomena were observed within the measurement accuracy given above. No further phase transitions were observed under compression up to 4.1 GPa (the highest pressure achieved in the experiment). The decompression brings the crystal to its initial state. The transformation spectra from 100 cm^{-1} to 600 cm^{-1} under compression are shown in Fig. S3. The changes in the middle wavenumber region is not considerable. Unfortunately, the lower wavenumber range is too noisy for analysis. The lines of the low-wavenumber region of the spectrum cannot be discussed accurately. We did not included these results in the paper.

Phase boundary dependence has been measured by Fokina *et al.*[4] up to a pressure of 0.6 GPa. Extrapolation of the boundary interface at a temperature of 295 K gives the phase transition pressure of 0.74 GPa. The difference between calculated and experimentally obtained data is 0.26 GPa, which is much larger than the experimental error of 0.05 GPa. Such discrepancy can be easily explained if one assumes the existence of a triple point. This assumption would also explain the different behavior of the spectral lines in phase high-pressure (Fig. 5) and low-temperature phase (Fig. 2).

Theoretical calculations

To consider the possible effects of $TiOF_5^{3-}$ groups ordering on crystal lattice dynamics and phase transition, their dynamics and statistics were simulated within *ab initio* generalized Gordon–Kim model. According to previous results[23,24] this model is unable to give a good quantitative agreement with experimental data yet it gives a reasonable qualitative description of phase transitions in different oxide and fluoride crystals.

Phonon spectra for several ordered phases of Rb_2KTiOF_5 have been simulated to interpret effects of lattice ordering on experimental vibrational spectrum. Crystal lattice of Rb_2KTiOF_5 with uniformly ordered $TiOF_5^{3-}$ ions has *I*4*mm* ($Z = 2$) structure, with vibrational representation

$$\Gamma = 7A_1 + A_2 + 2B_1 + 2B_2 + 9E$$

The Raman active modes are given in bold. Only one of these $\boldsymbol{A}_1$ modes appears in the high (800–1000 cm^{-1}) wavenumber range, which corresponds to Ti–O stretching, whereas at least three lines were observed experimentally in this range for both phases.

The crystal energy and phonon spectra at $k = 0$ were simulated for five other structures with different ordering of $TiOF_5^{3-}$ ions. Parameters of these structures and energies are given in Table 2, and highest wavenumbers are shown in Fig. S4. Several Ti–O stretching modes with close wavenumbers found for structure 1 are due to different site symmetries of these ions, while structures 2–4 have only one such mode each, but with slightly different frequencies.

We suggest that modes observed experimentally in the 850–950 cm^{-1} region correspond to stretching modes of Ti – O bond but their positions differ because of different site symmetries of

Table 2. Parameters of simulated structures with different packing of $TiOF_5^{3-}$ groups

Number of the structure	Cell parameters (a.u.)	Space group	*Z*	Direction of Ti–O bonds (bonds are considered in planes normal to *z* axis)	Energies (a.u.) per 1 formula unit
1	$a = b = c\sqrt{2} = 22.72$	*P*11*m*	8	$\pm x$, $\pm y$ in every plane	−7980.1523
2	$a = b = c = 16.07$	*P*11*m*	4	$\pm x$ and $\pm y$ directionsin neighboring planes	−7980.1677
3	$a = b = c = 16.07$	*Pmm*2	4	$\pm z$ in every plane	−7980.1676
4	$a = b = c = 16.07$	*P*4*mm*	4	all along *z* axis, +*z* and –*z* directions in neighboring planes	−7980.1599
5	$a = b = c/\sqrt{2} = 16.07$	*I*4*mm*	2	+*z* (polar phase)	−7980.1671

$TiOF_5^{3-}$ ions and different short range packing. Partial ordering of the structure below phase transition results in lines narrowing but not lines splitting. That could indicate a rather complex structure of low temperature phase (like our structure 1) with several close Ti–O lines, and with some elements of structural disorder.

The same ideas may be applied to low and medium wavenumber parts of the spectra, but it is more difficult to attribute experimental and calculated modes in these regions.

To simulate the ordering processes of $TiOF_5$ molecular groups, we use the same parameters of their interaction, taken from Table 2. Critical temperature was determined by Monte Carlo approach. Temperature dependence of heat capacity excess is shown in Fig. S5. We did not account for long range interactions in this simple model and as a result the calculated critical temperature of lattice ordering is much higher than the experimental one (above 1000 K). However, this model shows partial orientational ordering of $TiOF_5$ molecular groups in lower temperature phase. Structures 2 and 3 appear energetically most preferable; dipole moments of the molecular groups are oriented in the *xy* plane for structure 2, and in $\pm z$ direction for structure 3. Competition of these two types of ordering with very close energies results in partial disorder of low temperature phase. Compression of the structure disturbs this energy balance and leads to another partially ordered high pressure phase.

Conclusion

Raman spectra of Rb_2KTiOF_5 have been observed for the first time and analyzed in temperature range from 77 to 297 K and at pressures up to 4.1 GPa. The cubic phase was found to be orientationally disordered; such conclusion was reached based on the observed broadening of linewidths of internal vibrations far from the transition point. Comparison of experimental data with quantum-chemical calculation demonstrates that considerable changes in the Ti–O stretching vibration region are due to distortion of the $TiOF_5^{3-}$ octahedral and Rb^+ displacements. Temperature hysteresis of phase transition was observed; its value was measured to be about 6 K. Both experimental data and results of numerical simulations showed that these phase transitions results from orientational ordering of $TiOF_5$ groups lattice, but new phases stay partially disordered as well. This ordering manifests in a drastic narrowing of lattice vibration lines and in the appearance of new lines. At a pressure of 1 GPa, reversible structural phase transition was observed. Further increase of pressure up to 4.1 GPa did not show any effects associated with phase transitions. The differences in behavior of spectra transformations on temperature and high pressure indicates the presence of the triple point in the pressure range from 0.6 to 1 GPa.

Acknowledgements

This work was partly supported by integration project SB RAS No 101, Russian Foundation for Basic Research project No 11-02-98002-r_siberia, No 09-02-00062, SS-4645.2010.2.

The authors are indebted to Prof. I.N. Flerov for providing samples and for discussion of the results, V. D. Fokina for the useful discussions. The assistance of Victor Ouskin is highly appreciated.

Supporting information

Supporting information may be found in the online version of this article.

References

[1] K. Dehnike, G. Pausewang, W. Rudoff, *Z. Anal. Chem.* **1969**, *366*, 64.
[2] J. F. Scott, *Ann. Rev. Mater. Res.* **2011**, *41*, 1.
[3] J. F. Scott, R. Blinc, *J. Phys. Condens. Mat.* **2011**, *23*, 3202.
[4] V. D. Fokina, I. N. Flerov, M. S. Molokeyev, E. I. Pogoreltsev, E. V. Bogdanov, A. S. Krylov, A. F. Bovina, V. N. Voronov, N. M. Laptash, *Phys. Solid State* **2008**, *50*, 2175.
[5] E. I. Voigt, V. A. Davydov, A. A. Mashkovskii, A. V. Voigt, *J. Struct. Chem.* **2008**, *49*, 13.
[6] M. V. Gorev, I. N. Flerov, E. V. Bogdanov, V. N. Voronov, N. M. Laptash, *Phys. Solid State* **2010**, *52*, 167.
[7] M. V. Gorev, E. V. Bogdanov, I. N. Flerov, V. N. Voronov, N. M. Laptash, *Ferroelectrics* **2010**; *397*, 76.
[8] I. N. Flerov, M. V. Gorev, A. Tressaud, N. M. Laptash, *Crystallogr. Rep.* **2011**, *56*, 9.
[9] S. N. Krylova, A. N. Vtyurin, A. Belyu, A. S. Krylov, N. G. Zamkova, *Phys. Solid State* **2004**, *46*, 1311.
[10] A. S. Krylov, S. N. Krylova, A. N. Vtyurin, N. V. Surovtsev, S. V. Adishev, V. N. Voronov, A. S. Oreshonkov, *Crystallogr. Rep.* **2011**, *56*, 18.
[11] Yu. V. Gerasimova, A. S. Krylov, A. N. Vtyurin, N. M. Laptash, S. V. Goryainov, *Phys. Solid State* **2008**, *50*, 1534.
[12] N. M. Laptash, I. G. Maslennikova, T. A. Kaidalova, *J. Fluorine Chem.* **1999**, *99*, 133.
[13] I. N. Flerov, M. V. Gorev, V. D. Fokina, A. F. Bovina, N. M. Laptash, *Phys. Solid State* **2004**, *46*, 915.
[14] G. Blasse, G. J. Dirksen, *J. Solid State Chem.* **1990**, *88*, 586.
[15] A. N. Vtyurin, S. V. Goryainov, N. G. Zamkova, V. I. Zinenko, A. S. Krylov, S. N. Krylova, A. D. Shefer, *Phys. Solid State* **2004**, *46*, 1301.
[16] R. G. Munro, G. J. Piermarini, S. Block, W. B. Holzapfel, *J. Appl. Phys.* **1985**, *57*, 165.
[17] W. L. Vos, J. A. Schouten, *J. Appl. Phys.* **1991**, *69*, 6744.
[18] S. V. Goryainov, I. A. Belitsky, *Phys. Chem. Miner.* **1995**, *22*, 443.
[19] P. A. Jansson. Deconvolution with application in spectroscopy, Academic Press, Orlando, **1984**.
[20] M. W. Schmidt, K. K. Baldridge, J. A. Boatz *et al.*, *J. Comput. Chem.* **1993**, *14*, 1347.
[21] A. Slodczuk, Ph. Colomban, M. Pham-Thi, *J. Phys. Chem. Solids* **2008**, *69*, 2503.
[22] V. Ya Kavun, S. G. Kozlova, I. A. Tkachenko, S. P. Gabuda, *J. Struct. Chem.* **2010**, *51*, 463.
[23] V. I. Zinenko, N. G. Zamkova, S. N. Sofronova, *J. Exp. Theor. Phys.* **2003**, *123*, 747.
[24] V. I. Zinenko, S. N. Sofronova, *Ferroelectrics* **2004**, *307*, 25.